REVIEWER 1

We appreciate Reviewer 1 for his/her positive and constructive comments on the submitted manuscript. The following are our point-by-point responses to the reviewer's comments.

C1 - INTRODUCTION SECTION: In the introduction section, there is a lack of a description of the effects of the 26th December 2004 Indian Ocean Tsunami on the study area. Therefore, I suggest that the authors add a short paragraph in which they are invited to outline the reasons why the study area of Padang, Indonesia, escaped the destructive effects of the 26 December 2004 Indian Ocean tsunami.

Answer:

The main reason insignificant effects of the 2004 Indian Ocean tsunami in Padang areas is because the source location where the earthquake rupture occurred was far from Padang (i.e. >1,200 km). The 2004 source is centred in the Andaman segment of the Sunda subduction zone which is located in the north-west of Sumatra Islands (Meltzner et al., 2006; Briggs et al., 2006). On the other hand, Padang is located in the centre-west part of Sumatra and therefore, the 2004 tsunami events was not majorly affected this areas.

We added a short paragraph in Introduction describing the effects of the 2004 Indian Ocean tsunami to outline the 2004 Indian Ocean tsunami as follow:

The 2004 Aceh-Andaman tsunami did not significantly affect this region since the source location of the 2004 event was far, i.e. >1,200 km (Natawidjaja et al., 2006; Meltzner et al., 2006; Briggs et al., 2006). However, it is located along the coast of Sumatra Island, directly facing the Mentawai segment of the Sunda subduction zone. Consequently, potential impact of the future tsunami may be significant in this area. In addition, with the low-lying plain topographic features in Padang, the probability of large inundated areas and large inundation depths is also high (Borrero et al., 2006; Muhari et al., 2010, 2011).

C2 - EARTHQUAKE SCENARIO SELECTION: The authors must justify their choice as regards the magnitudes of the earthquake scenarios. Why a minimum Magnitude of 8.5 and not 8.25, for instance? Is a Mw8.25 earthquake causes a tsunami with no significant effect on the study area? Why do the authors not consider a maximum earthquake magnitude in the range of this of the 2004 Indian Ocean event (Mw9.2)? Such a choice would change the predicted tsunami inundation characteristics and therefore the associated evacuation plan.

Answer:

We used M_w 8.5 as the minimum scenario magnitude in our study because the tsunami hazard produced from the magnitudes less than this level, e.g. M_w 8.25 and M_w 8.0, are considered to be relatively small (below 1 m wave height in the coastal areas; McCloskey et al., 2008; Muhammad et al., 2016). From Figure 1 in this document, we see the relatively minor effects in Padang due to M_w 8.5 tsunami . It shows the tsunami wave heights at three stations, i.e. Tabing, Purus, and Teluk Bayur, at a depth of 5 m. The median wave heights produced from 100 tsunamigenic scenarios are about 1 m which is small and will have minor impact on land (see Muhammad et al., 2016). The impact becomes more insignificant if we consider the M_w 8.25 scenario. Therefore, we choose the M_w 8.5 as the minimum magnitude scenarios.

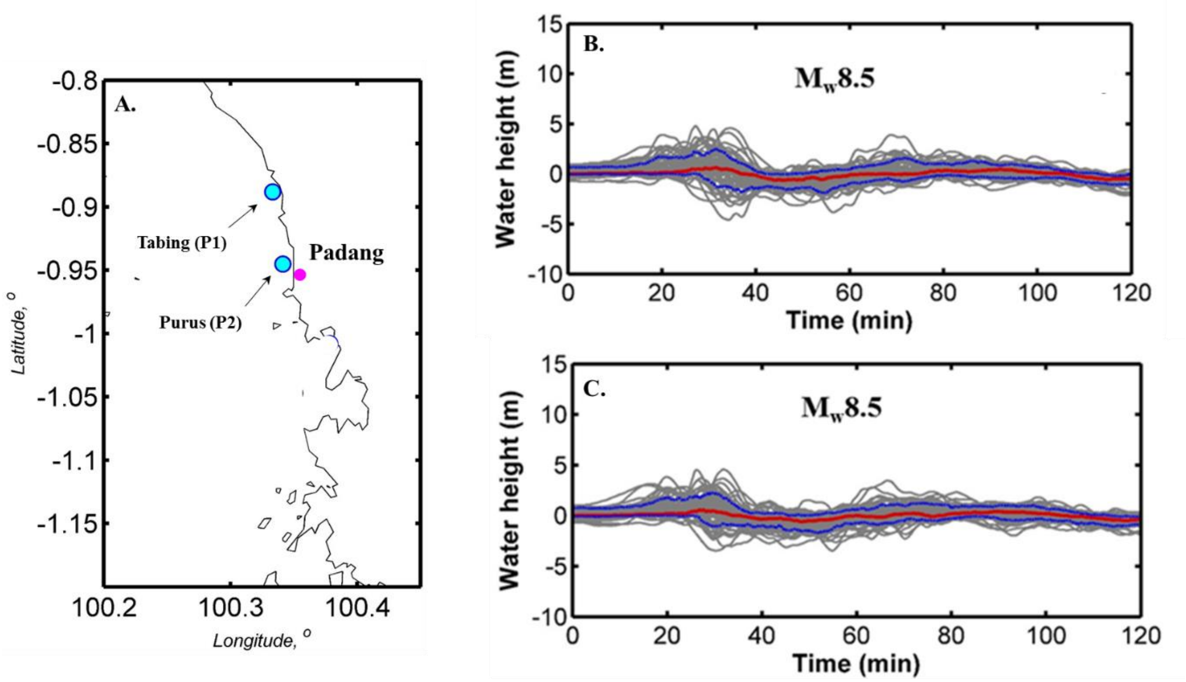

Figure 1. Tsunami wave height profile near coastal line of Padang: (A) site location. (B). Tabing (P1) station). (C). Purus (P2) station.

For the maximum scenarios (i.e. M_w 9.0), it was selected based on the existing research studies from geodetic, paleogeodetic, and paleotsunami investigations. These studies indicated that the accumulated slip in the Mentawai segment of the Sunda subduction zone may generate the tsunamigenic earthquake with the magnitude ranging from M_w 8.8 to M_w 9.0 (Zachariasen et al., 1999; Natawidjaja et al., 2006; Sieh et al., 2008). We did not consider a extreme scenario like the 2004 Indian Ocean tsunami (which is very long) because the tsunami sediment records in North of Sumatra indicated that the recurrence time of destructive tsunamis from the Aceh-Andaman sources is at least 600 years in comparison to ~200 years for the Mentawai segment

(Natawidjaja et al., 2006; Monecke et al., 2008) and hence, the M_w 9.0 consider to be more likely than the scenarios such as the 2004 Indian Ocean tsunami. However, such long ruptures are a possibility in the Mentawai segment – we simply did not consider such an assumption.

Based on Reviewer's recommendations, we have added to the methodology section of the revised manuscript the following descriptions regarding the choice of our magnitude scenarios in the revised manucript as follows:

The magnitude M_w 8.5 is used as the minimum scenario because the tsunami hazard produced from the magnitude below this level, e.g. M_w 8.25 and Mw 8.0, is relatively small (less than 1 m wave height in the coastal areas; see Muhammad et al., 2016). The maximum magnitude scenario (M_w 9.0) is selected based on geodetic, paleo-geodetic, and paleo-tsunami studies (Zachariasen et al., 1999; Natawidjaja et al., 2006; Sieh et al., 2008); they indicated that the accumulated slip in the Mentawai segment of the Sunda subduction zone may generate the tsunamigenic earthquake with the magnitude range from M_w 8.8 to M_w 9.0.

C3 - STOCHASTIC TSUNAMI SIMULATION: It is not clear in the text that the numerical model used in this study is a finite-difference code solving non-linear shallow water equations in the Cartesian coordinate system. Please clarify. Also, I suppose that the numerical tsunami code (Goto et al., 1997) was benchmarked and used to accurately simulate other tsunami events, thereby, the authors should mention some references on this. Which algorithm was used to track the shoreline movement and calculate the inundation? Is it the moving boundary algorithm (Liu et al., 1995)? Other?

Answer:

Yes it is. We used a finite-difference code to numerically solve non-linear shallow water equations in the Cartesian coordinate system.

We have added several references to the revised manuscript regarding the implementation of Goto et al. (1997) model for tsunami simulation.

The algorithm to track the shoreline movement and calculate the inundation is using approximate moving boundary algorithm proposed by Iwasaki and Mano (1797).

To cover the recommendations from the reviewer, the following texts have been added into the revised manuscript:

A finite-difference method implementing a staggered leap-frog scheme is adopted to solve the governing equations (Goto et al., 1997). In addition, in Goto et al.'s code the moving boundary approach developed by Iwasaki and Mano (1979) is used for inundation modeling. This method has been successfully used to run the tsunami simulation in several regions, including Padang, Indonesia, Mexico, and Japan (Muhari et al., 2010, 2011; Goda et al., 2014; Mori et al., 2017).

C4 - METHOD FOR THE DEVELOPMENT OF EVACUATION PLANS: The paper addresses the development of tsunami evacuation plans using high-resolution flood maps and compares the estimated inundation depths with the buildings heights to define the vertical evacuation shelters. In my opinion, a crucial component for the development of effective evacuation plans is missing in this approach. It consists of investigating the vulnerability of the coastal building located within the inundation zone, in particular, the buildings assessed as shelters. This must include an assessment of the buildings resistance capacity to a successive impact of both the earthquake and the tsunami. The study site is located within the co-seismic deformation area (Fig. 1 and 3) and, therefore, a Mw8.5-9.0 earthquake would cause a strong shaking that can have heavy damage on the coastal buildings and road network well before the arrival of the tsunami wave. This issue must be addressed for an effective planning of tsunami evacuation in Padang, Indonesia.

Answer:

Thank you very much for these valuable comments. We have re-assessed the vulnerability of tsunami evacuation shelters (TES) considering both seismic and tsunami loadings. A new section **Section 2.2. vulnerability assessment of tsunami evacuation shelters** has been added in the methodology section of the revised manuscript to explain the shaking and tsunami vulnerability assessments. The results from these assessments are also included in the results and discussion section. To facilitate the communications with the editor and the reviewers, a summary of the TES vulnerability assessment procedure and the assessments results is detailed in the following.

PROCEDURE OF SHAKING AND TSUNAMI VULNERABILITY ASSESSMENTS OF TSUNAMI EVACUATION SHELTERS

A procedure to carry out vulnerability assessments of TESs due to shaking and tsunami is presented in Figure 2. First, earthquake and tsunami simulations are conducted. A ground motion prediction equations (GMPE) developed by Abrahamson et al. (2016) is adopted to carry out the earthquake simulation (see in the revised manuscript section 2.2.1). Noted that, the source scenarios for the seismic and tsunami simulations are the same. Second, the vulnerability assessment is carried out. The building vulnerability is assessed by determining the probability of a building experiencing specific damage states for a given hazard level, e.g. spectral acceleration (Sa) at a certain vibration period and spectral displacement for shaking and maximum tsunami depth (h) for tsunami (Rossetto and Elnashai, 2003; De Risi and Goda, 2016). Subsequently, the fragility models for both earthquake and tsunami vulnerability assessment are adopted. Since the tsunami is a secondary hazard triggered by an earthquake fault rupture, the seismic vulnerability assessment of TESs is carried out prior to the tsunami vulnerability assessment (see Figure 2). In this study, the combined effects of earthquake shaking and tsunami are not taken into account, because such multi-hazard fragility models are not available for TES in Padang. Detail procedures for the TES earthquake-tsunami hazard and vulnerability assessments are presented below.

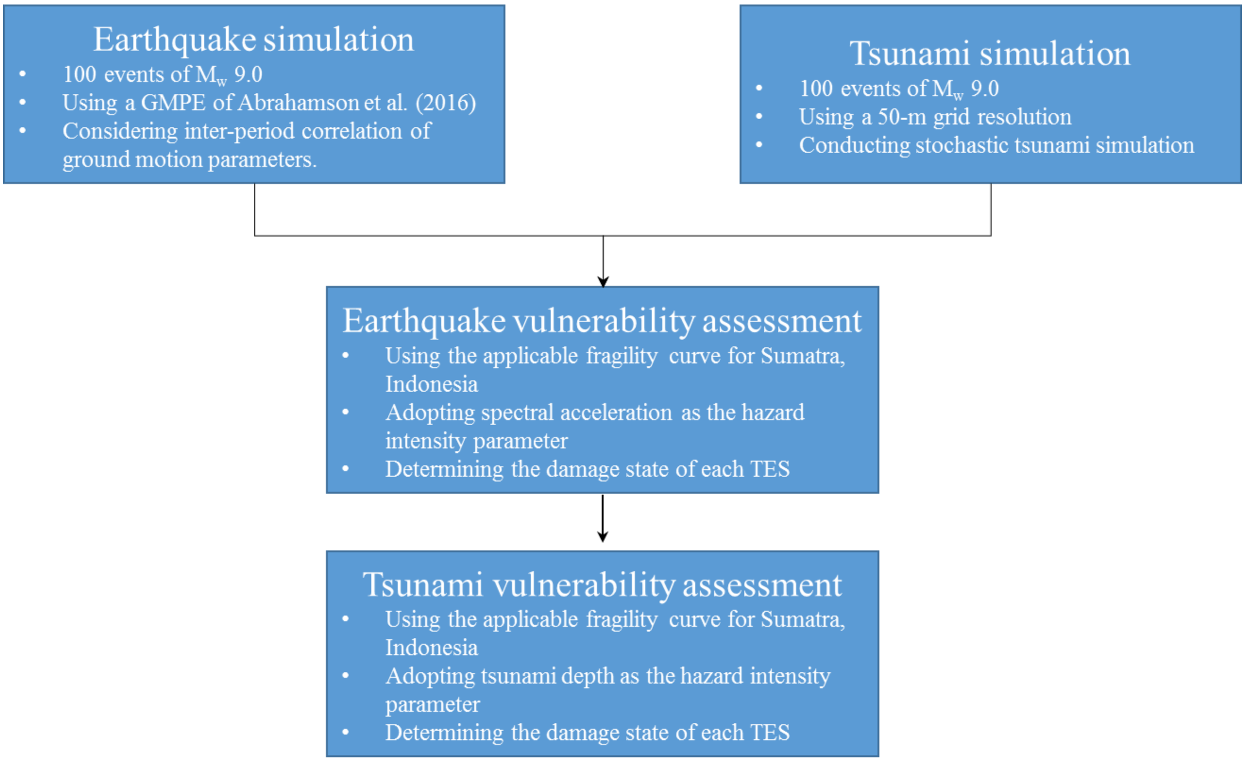

Figure 2. Procedure of earthquake and tsunami hazard and vulnerability assessment of tsunami evacuation shelters.

For seismic vulnerability assessment, the fragility curves developed by Federal Emergency Management Agency (FEMA), i.e. HAZUS, is adopted to assess the vulnerability of TESs in Padang because of the following reasons:

1. The TES are designed and constructed according to the new Indonesian Earthquake Resistance Building Code (SNI-1726: 2012) adopting the U.S. seismic design documents, i.e. FEMA P750 (2009), regarding seismic design provisions for new building and other structures, and ASCE/SEI 7-10 for the minimum design load criterion (SNI-1726: 2012; Kurniawan et al., 2014; Wijayanti et al., 2015; Aulia, 2016; Sengara et al., 2016).
2. HAZUS is a well-established earthquake loss estimation framework and has been implemented in several earthquake-prone countries for seismic risk assessment purposes, e.g., Haiti, Puerto Rico, France, Romania, Austria, and Indonesia (Kulmesh, 2010; Peterson and Small, 2012; Wijayanti et al., 2015; Sengara et al., 2016).

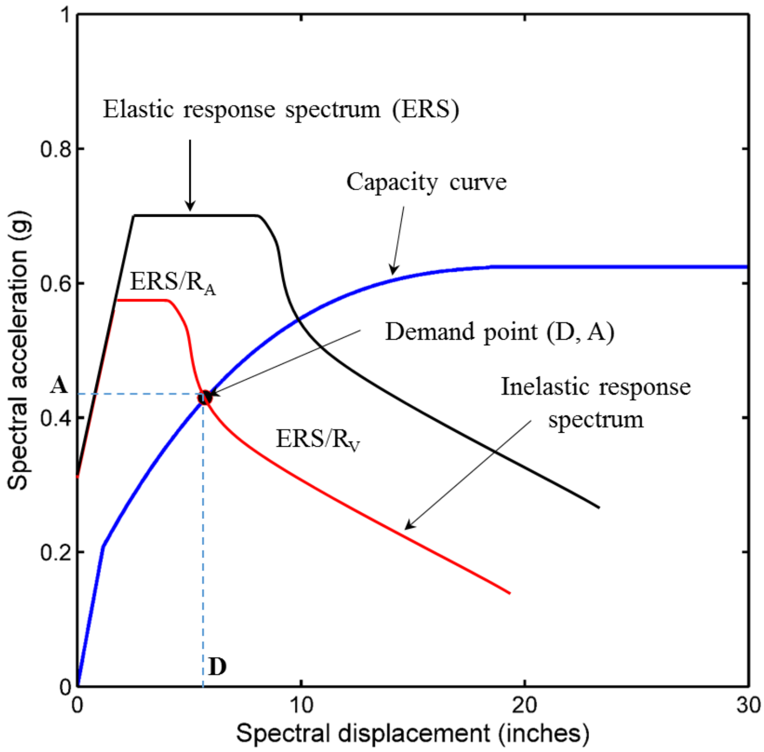

Figure 3. Example of Capacity Spectrum Method.

Figure 3 illustrates the procedure for developing an inelastic response (demand) spectrum from the elastic response (input) spectrum in HAZUS. First, the acceleration response spectrum is generated from the earthquake simulation (see in the revised manuscript Section 2.2.1), and is further converted into the acceleration-displacement response spectrum (ADRS). In the CSM, the ADRS is defined as the elastic response spectrum (ERS). Second, the inelastic demand spectrum is calculated by dividing the ERS by the reduction factors (i.e. R_A at periods of constant acceleration and R_V at periods of constant velocity). Note that the reduction factors in HAZUS are equal to the reciprocal of SR_A and SR_V in ATC-40 (ATC, 1996). For essential and average buildings (type B), the SR_A and SR_V should be less than 2.27 and 1.79, respectively (ATC, 1996). On the other hand, the TES may be classified as type B based on the ATC-40 system and hence, R_A and R_V should be less than 2.27 and 1.79, respectively. In this study, both R_A and R_V are set to 1.5 (Lin and Chang, 2003; Casarotti et al., 2009; Monteiro et al., 2014). Third, the capacity curve taken from HAZUS is overlaid to compare with the inelastic response spectrum (see blue line in Figure 3A). The capacity curve in HAZUS is defined based on two parameters, e.g. yield and ultimate strengths characterizing the nonlinear (pushover) behavior. The building-type classifications in HAZUS are based on the building material (e.g. wood, reinforced concrete and steel) and height. Following the HAZUS classification, the TES in Padang is categorized as reinforced concrete moment resistant frames (RC-MRF) with different building heights. TES numbers 13 and 16 are high-rise RC-MRF (C1H), whereas the rest of TES are mid-rise RC-MRF (C1M). Moreover, in HAZUS, four seismic design codes classification including Pre-Code, Low-Code, Moderate-Code, and High-Code are defined corresponding to the seismic zone. In terms of seismic design code classification, High-Code is applicable to TES in Padang, because Padang is located in the high seismic zone and TES has been designed and constructed to higher standards/quality than other normal buildings (Kurniawan et al., 2014; Aulia, 2016). In the following, the seismic vulnerability assessment of TES is carried out by focusing upon C1M because the C1H type is typically stronger than C1M in terms of capacity curve (i.e. for the same shaking intensity, CH1 buildings are expected to perform better than CM1).

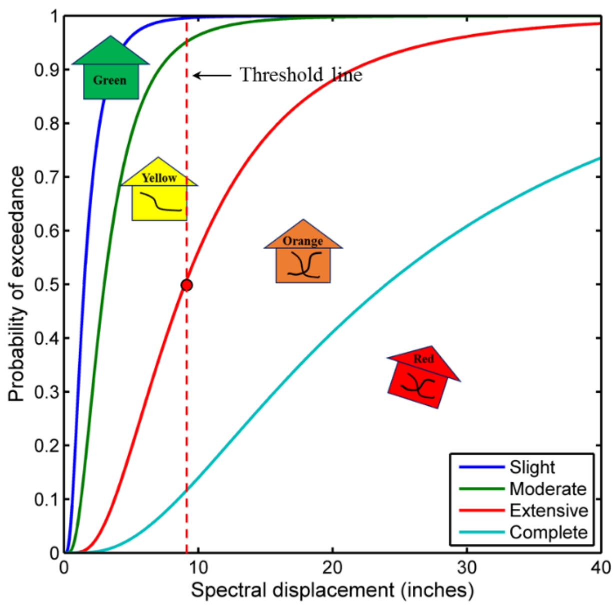

Figure 4. Fragility curves developed in HAZUS-MH (2001).

Finally, seismic fragility curves implemented in HAZUS are used to define the damage functions of the building; typically, the fragility functions are defined using the lognormal distribution. Subsequently, to determine whether a TES can be used for post-earthquake tsunami evacuation purposes (not for shelters), the building is categorized into safe and unsafe by referring to existing tagging criteria (FEMA 356, 2000; HAZUS, 2003; Bazzurro et al., 2006) including (see Figure 4):

- Green tag: the building may have experienced onset damage but is safe for immediate occupancy. The none-to-slight damage state is applicable.
- Yellow tag: re-occupancy of the building is restricted and limited access only is allowed. Moderate-to-extensive damage state corresponds to this case.
- Red tag: the building is unsafe and no access is granted, and will be in complete damage or collapse state.

Based on the above tagging criteria, the tsunami evacuation building may be judged as unsafe for evacuation if the probability of extensive and complete damage states is over 50%. This assumption gives a 50-50 chance that the building may experience above or below extensive damage (Bazzurro et al., 2006). Moreover, the 50% probability of extensive or severer damage state is typically identified as the threshold value of a yellow tag in HAZUS that is adopted in this study (see Figure 4) and hence, may be regarded as the limit state to define the accessibility of buildings for emergency evacuation during the tsunami inundation

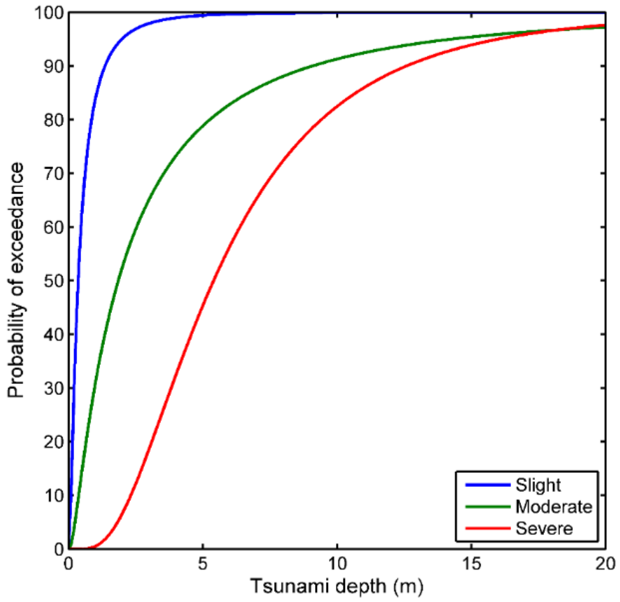

Figure 5. Tsunami fragility models developed by Suppasri et al. (2011)

For tsunami vulnerability assessment, the model by Suppasri et al. (2011) is adopted for the following reasons. It was developed through extensive remote sensing and tsunami survey data (i.e. ~5,000 points) in Banda Aceh and Thailand for the 2004 Aceh-Andaman tsunami, and is the most recent model among existing tsunami fragility models that are applicable to Sumatra, Indonesia. These features are important because current situations of tsunami mitigation measures in Padang resemble those in Banda Aceh and Thailand more closely than situations in other regions. The Suppasri et al. model considers three damage states for tsunami damage (see Figure 5) and consists of three fragility curves for reinforced concrete building for slight (DST1), moderate (DST2), and major/severe damage state (DST3). Using the calculated probability exceedance of each damage state, the TES is considered to be unsafe if the exceedance probability of severe damage is above 50% (the major tsunami damage is assumed to be similar to the extensive damage in seismic damage state criteria).

RESULTS

For seismic vulnerability assessment, first, the earthquake-HAZUS vulnerability assessment using the median response spectra of the worst cases (i.e. M_w 9.0 and R = 55 km) is presented in Figure 6 as an illustration of the seismic-HAZUS vulnerability assessment framework. Note that this response spectrum does not include the inherent uncertainty associated with the earthquake ground motion simulation. The ADRS for this case is further calculated and shown as a blue line in Figure 6B. Using the ADRS, the CSM is implemented to determine the performance (demand) point (Figure 6C). After applying the reduction factors to obtain an inelastic seismic demand spectrum (green line in Figure 6C), the performance point is estimated to be about 3 inches (7.6 cm) and then used to calculate the probability exceedance of damage states for a TES. Figure 6D shows that the sum of probabilities for extensive and complete damage states is ~7% and hence, the TES is considered to be safe for the median response spectra of the worst case.

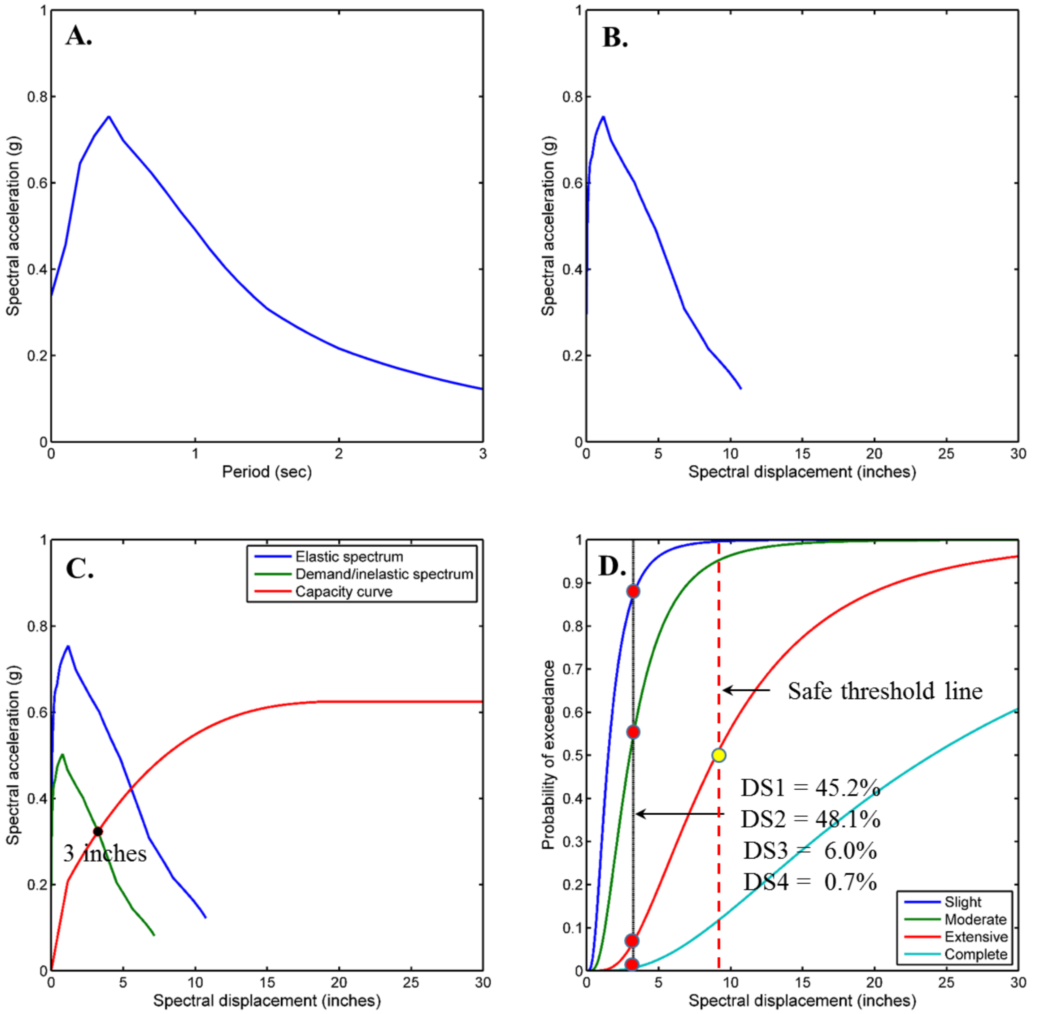

Figure 6 the seismic-HAZUS TES vulnerability assessment using the worst scenario.

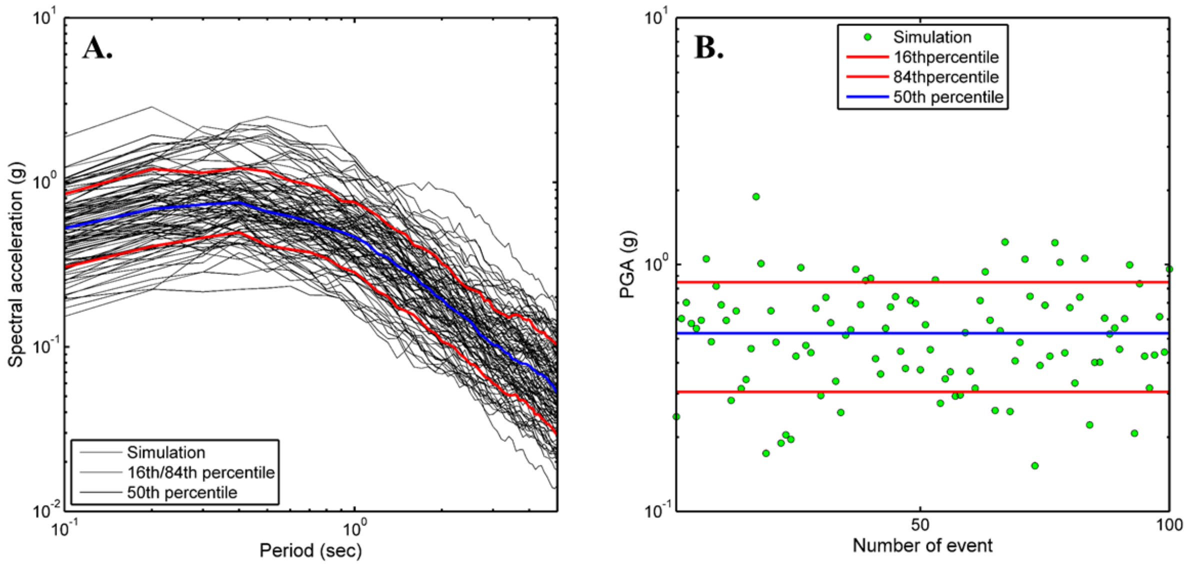

Figure 7. Earthquake simulation results from 100 tsunamigenic scenarios: (A). Spectral acceleration. (B). Peak Ground Acceleration (PGA).

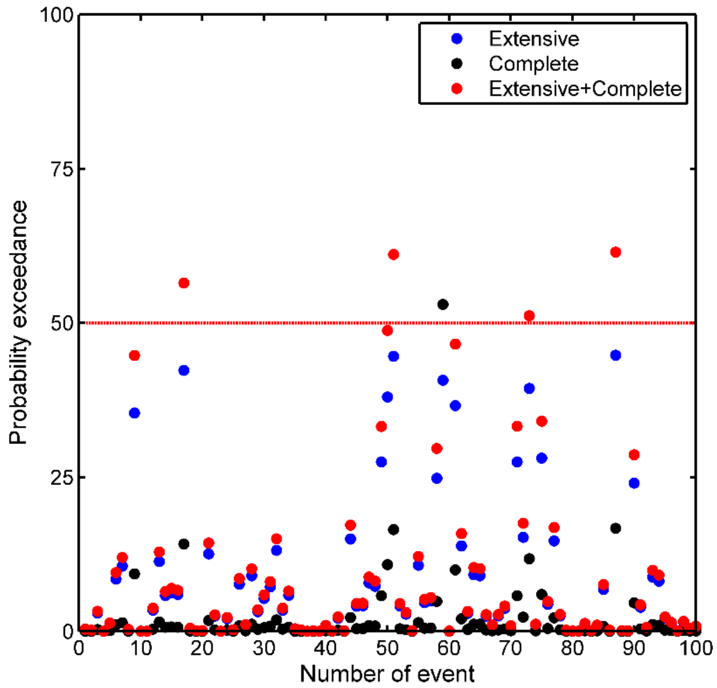

Figure 8. Probability exceedance of extensive and complete damage states for 100 seismic events.

The assessment that is illustrated in Figure 6 ignores the inherent uncertainty of input ground motions. To account for this uncertainty, ground motion simulation results for 100 tsunamigenic earthquake scenarios are presented in Figure 7 by considering the prediction error terms of the ground motion model together with inter-period correlations. The spectral acceleration profiles show a range of ground shaking that is expected to occur in Padang due to the 100 tsunamigenic earthquakes generated from the Mentawai segment of the Sunda subduction zone. The range of Sa in Padang is between 0.2 g to 1.1 g for the period below 1 s (Figure 7A). Moreover, the PGA values (Figure 7B) is at the interval of 0.3 g to 0.9 g with the median of about 0.5 g. Using the simulated response spectra from those 100 earthquake scenarios, the TES vulnerability is assessed. Figure 8 presents the three kinds of exceedance probability of damage states; blue dots correspond to extensive damage state, black dots correspond to complete damage state, and red dots represent the sum of these two probabilities. A 50% probability line is drawn to indicate the threshold of safe building that is considered in this study. Figure 8 indicates that the TES may be operational for evacuation because ~95% from the total of 100 earthquake simulations produce less than 50% exceedance probability of the combined extensive-complete damage states. Moreover, most of the cases result in less than

25% probability of exceedance above the extensive damage state. Subsequently, the TES may be considered to be safe for evacuation after the ground shaking and hence, the tsunami vulnerability assessment can be carried out.

Fourth, the tsunami vulnerability assessment is performed. Using the maximum inundation depths at all 23 TES from the 100 earthquake scenarios of the M_w 9.0, the probability of exceeding the severe damage state (DST3) for each TES is calculated. When the chance of severe tsunami damage exceeds 50%, the TES is considered to be not usable as tsunami evaluation building. The probabilities of severe damage for the shelter numbers 16 and 17 are relatively large, i.e. 30% and 36% of the 100 events, and hence, these two shelters may be considered to be unsafe for the evacuation. Moreover, the probabilities of severe damage for the other shelters are relatively small (less than 25%). Therefore, except for the shelter numbers 16 and 17, the rest of the shelters are considered to be operational for evacuation.

Subsequently, the estimation of TES building capacity is evaluated. This may capture another point of view regarding the adequacy of existing TES for evacuation. In terms of capacity, except for shelters numbers 16 and 17, all TES buildings can be used for vertical evacuation during the 10^{th} rank event. However, for the 50^{th} percentile case, the shelter number 1 (sport center of UNP) may not be operational, whilst for the 90^{th} percentile case, shelter numbers 1 and 15 (Elementary school of 24 Padang) are unable to accommodate evacuees since all floors will be inundated. Note that, for the shelter number 1, there is only one floor since most of the building areas are used for the sport arena. In terms of capacity, for the 50^{th} and 90^{th} rank cases, the possible maximum capacity to be accommodated at all TES buildings are only about 64,000 and 41,000 people, respectively. These numbers are insufficient in comparison to the total population in the coastal region of Padang (i.e. ~200,000 people). Therefore, it is highly recommended to increase the number of TES near the coastal areas in Padang. Importantly, the TES assessment results highlight that the stochastic tsunami simulation method is able to capture the uncertainty of the future tsunamigenic impacts and hence, is essential to use this method for developing an effective tsunami mitigation plan.

C5 - RESULTS: The results of tsunami hazard assessment (inundation maps) are of good quality and reflect, On the other hand, results on evacuation plans must be reassessed taking into account the comment #4.

C6 - DISCUSSION: The discussion must be reworked on the light of the new results and include the vulnerability of the shelters to a successive impact from the earthquake and then the tsunami.

Answer C5 and C6:

We have incorporated the seismic and tsunami vulnerability assessment results to the results and discussion section.

REVIEWER 2

We highly appreciated the constructive comments given by the reviewer 2 for our submitted manuscript. The following are detail response of the reviewers comments.

C1: When dealing with building vertical evacuation, is it also considered the possibility of building collapses due to the earthquake itself? Such major earthquake often have considerable effects on edifice stability and integrity.

Answer:

Agreed. Considering the reviewer recommendations, we have re-assessed the vulnerability of tsunami evacuation shelters (TES) considering both seismic and tsunami loadings. A new section **Section 2.2. vulnerability assessment of tsunami evacuation shelters** has been added in the methodology section of the revised manuscript to explain the shaking and tsunami vulnerability assessments. The results from these assessments are also included in the results and discussion section. To facilitate the communications with the editor and the reviewers, a summary of the TES vulnerability assessment procedure and the assessments results is detailed in the following.

PROCEDURE OF SHAKING AND TSUNAMI VULNERABILITY ASSESSMENTS OF TSUNAMI EVACUATION SHELTERS

A procedure to carry out vulnerability assessments of TESs due to shaking and tsunami is presented in Figure 2. First, earthquake and tsunami simulations are conducted. A ground motion prediction equations (GMPE) developed by Abrahamson et al. (2016) is adopted to carry out the earthquake simulation (see in the revised manuscript section 2.2.1). Noted that, the source scenarios for the seismic and tsunami simulations are the same. Second, the vulnerability assessment is carried out. The building vulnerability is assessed by determining the probability of a building experiencing specific damage states for a given hazard level, e.g. spectral acceleration (Sa) at a certain vibration period and spectral displacement for shaking and maximum tsunami depth (h) for tsunami (Rossetto and Elnashai, 2003; De Risi and Goda, 2016). Subsequently, the fragility models for both earthquake and tsunami vulnerability assessment are adopted. Since the tsunami is a secondary hazard triggered by an earthquake fault rupture, the seismic vulnerability assessment of TESs is carried out prior to the tsunami vulnerability assessment (see Figure 2). In this study, the combined effects of earthquake shaking and tsunami are not taken into account, because such multi-hazard fragility models are not available for TES in Padang. Detail procedures for the TES earthquake-tsunami hazard and vulnerability assessments are presented below.

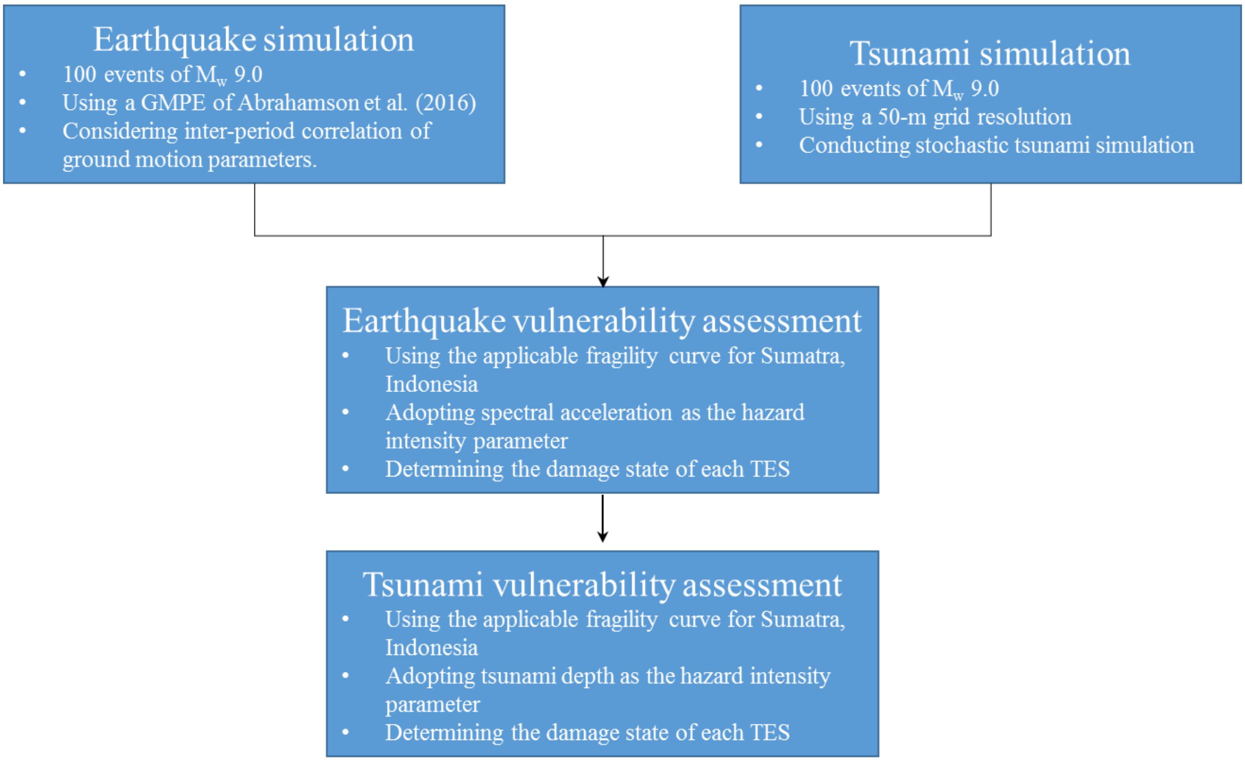

Figure 9. Procedure of earthquake and tsunami hazard and vulnerability assessment of tsunami evacuation shelters.

For seismic vulnerability assessment, the fragility curves developed by Federal Emergency Management Agency (FEMA), i.e. HAZUS, is adopted to assess the vulnerability of TESs in Padang because of the following reasons:

3. The TES are designed and constructed according to the new Indonesian Earthquake Resistance Building Code (SNI-1726: 2012) adopting the U.S. seismic design documents, i.e. FEMA P750 (2009), regarding seismic design provisions for new building and other structures, and ASCE/SEI 7-10 for the minimum design load criterion (SNI-1726: 2012; Kurniawan et al., 2014; Wijayanti et al., 2015; Aulia, 2016; Sengara et al., 2016).
4. HAZUS is a well-established earthquake loss estimation framework and has been implemented in several earthquake-prone countries for seismic risk assessment purposes, e.g., Haiti, Puerto Rico, France, Romania, Austria, and Indonesia (Kulmesh, 2010; Peterson and Small, 2012; Wijayanti et al., 2015; Sengara et al., 2016).

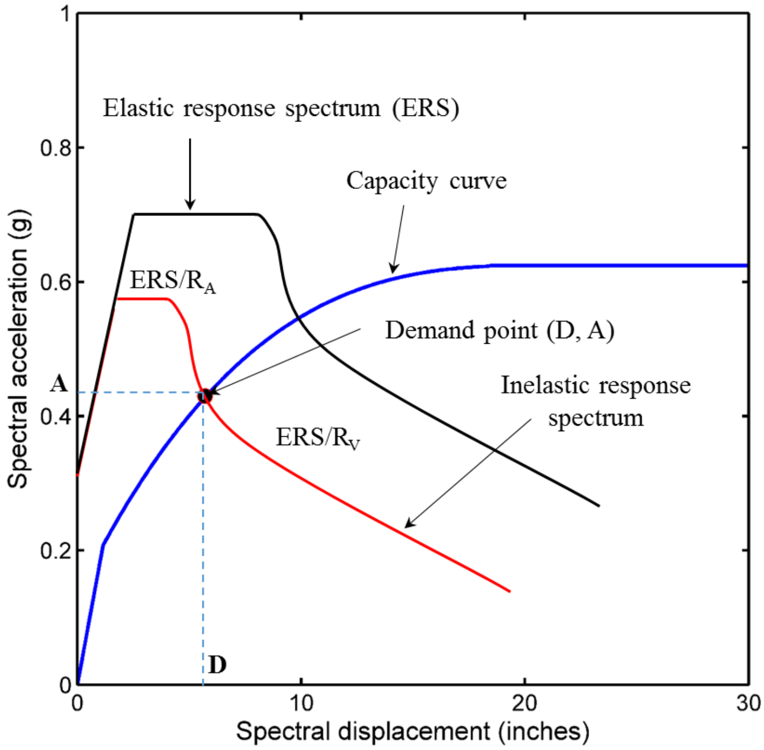

Figure 10. Example of Capacity Spectrum Method.

Figure 3 illustrates the procedure for developing an inelastic response (demand) spectrum from the elastic response (input) spectrum in HAZUS. First, the acceleration response spectrum is generated from the earthquake simulation (see in the revised manuscript Section 2.2.1), and is further converted into the acceleration-displacement response spectrum (ADRS). In the CSM, the ADRS is defined as the elastic response spectrum (ERS). Second, the inelastic demand spectrum is calculated by dividing the ERS by the reduction factors (i.e. R_A at periods of constant acceleration and R_V at periods of constant velocity). Note that the reduction factors in HAZUS are equal to the reciprocal of SR_A and SR_V in ATC-40 (ATC, 1996). For essential and average buildings (type B), the SR_A and SR_V should be less than 2.27 and 1.79, respectively (ATC, 1996). On the other hand, the TES may be classified as type B based on the ATC-40 system and hence, R_A and R_V should be less than 2.27 and 1.79, respectively. In this study, both R_A and R_V are set to 1.5 (Lin and Chang, 2003; Casarotti et al., 2009; Monteiro et al., 2014). Third, the capacity curve taken from HAZUS is overlaid to compare with the inelastic response spectrum (see blue line in Figure 3A). The capacity curve in HAZUS is defined based on two parameters, e.g. yield and ultimate strengths characterizing the nonlinear (pushover) behavior. The building-type classifications in HAZUS are based on the building material (e.g. wood, reinforced concrete and steel) and height. Following the HAZUS classification, the TES in Padang is categorized as reinforced concrete moment resistant frames (RC-MRF) with different building heights. TES numbers 13 and 16 are high-rise RC-MRF (C1H), whereas the rest of TES are mid-rise RC-MRF (C1M). Moreover, in HAZUS, four seismic design codes classification including Pre-Code, Low-Code, Moderate-Code, and High-Code are defined corresponding to the seismic zone. In terms of seismic design code classification, High-Code is applicable to TES in Padang, because Padang is located in the high seismic zone and TES has been designed and constructed to higher standards/quality than other normal buildings (Kurniawan et al., 2014; Aulia, 2016). In the following, the seismic vulnerability assessment of TES is carried out by focusing upon C1M because the C1H type is typically stronger than C1M in terms of capacity curve (i.e. for the same shaking intensity, CH1 buildings are expected to perform better than CM1).

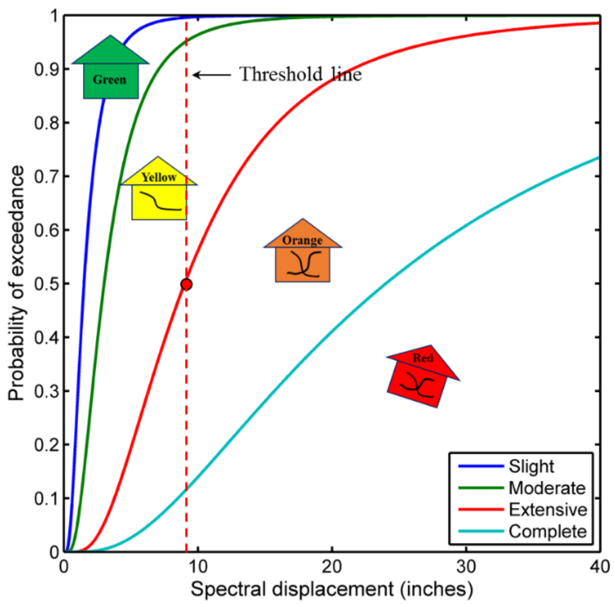

Figure 11. Fragility curves developed in HAZUS-MH (2001).

Finally, seismic fragility curves implemented in HAZUS are used to define the damage functions of the building; typically, the fragility functions are defined using the lognormal distribution. Subsequently, to determine whether a TES can be used for post-earthquake tsunami evacuation purposes (not for shelters), the building is categorized into safe and unsafe by referring to existing tagging criteria (FEMA 356, 2000; HAZUS, 2003; Bazzurro et al., 2006) including (see Figure 4):

- Green tag: the building may have experienced onset damage but is safe for immediate occupancy. The none-to-slight damage state is applicable.
- Yellow tag: re-occupancy of the building is restricted and limited access only is allowed. Moderate-to-extensive damage state corresponds to this case.

- Red tag: the building is unsafe and no access is granted, and will be in complete damage or collapse state.

Based on the above tagging criteria, the tsunami evacuation building may be judged as unsafe for evacuation if the probability of extensive and complete damage states is over 50%. This assumption gives a 50-50 chance that the building may experience above or below extensive damage (Bazzurro et al., 2006). Moreover, the 50% probability of extensive or severer damage state is typically identified as the threshold value of a yellow tag in HAZUS that is adopted in this study (see Figure 4) and hence, may be regarded as the limit state to define the accessibility of buildings for emergency evacuation during the tsunami inundation

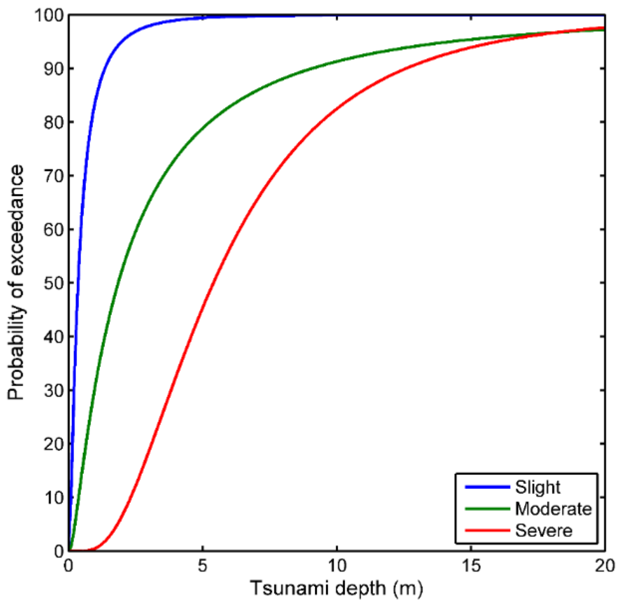

Figure 12. Tsunami fragility models developed by Suppasri et al. (2011)

For tsunami vulnerability assessment, the model by Suppasri et al. (2011) is adopted for the following reasons. It was developed through extensive remote sensing and tsunami survey data (i.e. ~5,000 points) in Banda Aceh and Thailand for the 2004 Aceh-Andaman tsunami, and is the most recent model among existing tsunami fragility models that are applicable to Sumatra, Indonesia. These features are important because current situations of tsunami mitigation measures in Padang resemble those in Banda Aceh and Thailand more closely than situations in other regions. The Suppasri et al. model considers three damage states for tsunami damage (see Figure 5) and consists of three fragility curves for reinforced concrete building for slight (DST1), moderate (DST2), and major/severe damage state (DST3). Using the calculated probability exceedance of each damage state, the TES is considered to be unsafe if the exceedance probability of severe damage is above 50% (the major tsunami damage is assumed to be similar to the extensive damage in seismic damage state criteria).

RESULTS

For seismic vulnerability assessment, first, the earthquake-HAZUS vulnerability assessment using the median response spectra of the worst cases (i.e. M_w 9.0 and R = 55 km) is presented in Figure 6 as an illustration of the seismic-HAZUS vulnerability assessment framework. Note that this response spectrum does not include the inherent uncertainty associated with the earthquake ground motion simulation. The ADRS for this case is further calculated and shown as a blue line in Figure 6B. Using the ADRS, the CSM is implemented to determine the performance (demand) point (Figure 6C). After applying the reduction factors to obtain an inelastic seismic demand spectrum (green line in Figure 6C), the performance point is estimated to be about 3 inches (7.6 cm) and then used to calculate the probability exceedance of damage states for a TES. Figure 6D shows that the sum of probabilities for extensive and complete damage states is ~7% and hence, the TES is considered to be safe for the median response spectra of the worst case.

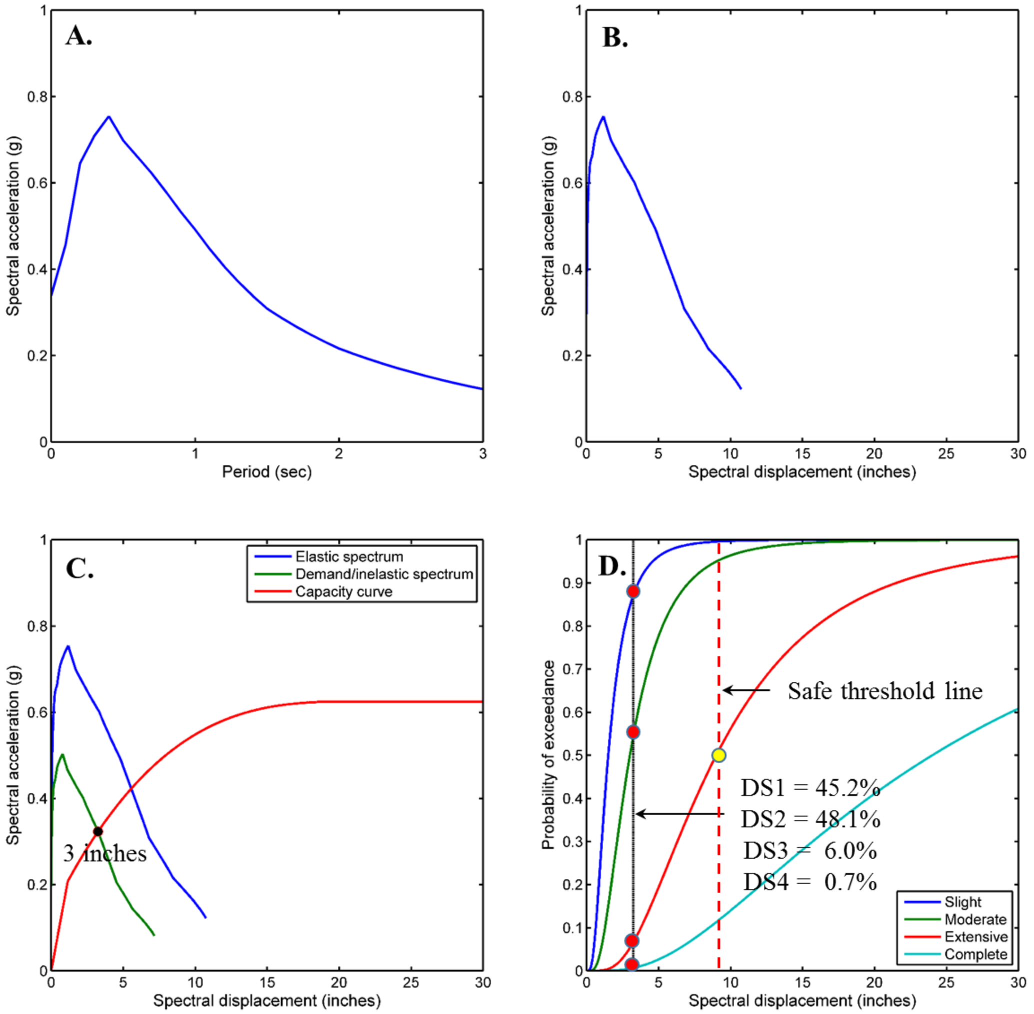

Figure 13 the seismic-HAZUS TES vulnerability assessment using the worst scenario.

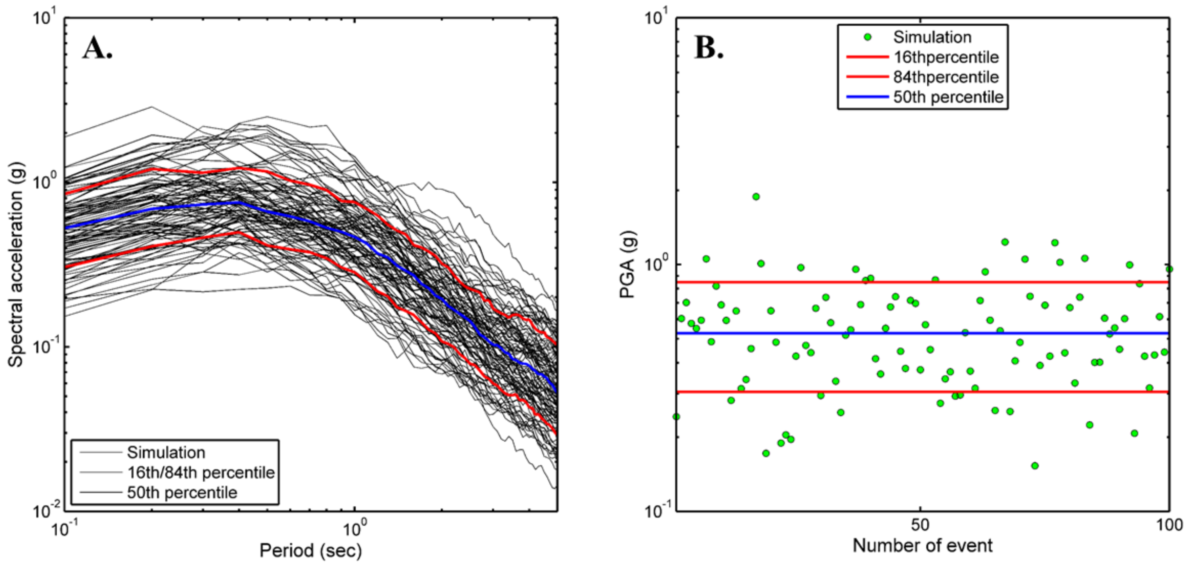

Figure 14. Earthquake simulation results from 100 tsunamigenic scenarios: (A). Spectral acceleration. (B). Peak Ground Acceleration (PGA).

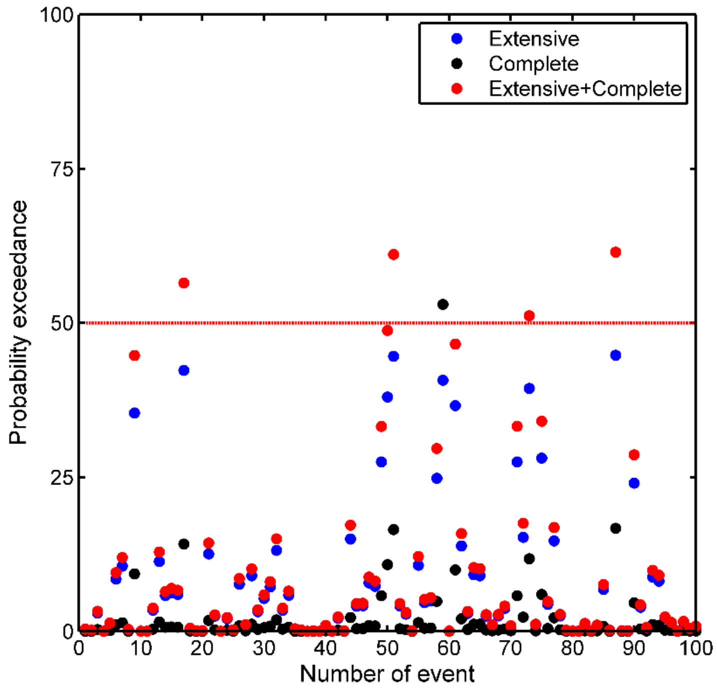

Figure 15. Probability exceedance of extensive and complete damage states for 100 seismic events.

The assessment that is illustrated in Figure 6 ignores the inherent uncertainty of input ground motions. To account for this uncertainty, ground motion simulation results for 100 tsunamigenic earthquake scenarios are presented in Figure 7 by considering the prediction error terms of the ground motion model together with inter-period correlations. The spectral acceleration profiles show a range of ground shaking that is expected to occur in Padang due to the 100 tsunamigenic earthquakes generated from the Mentawai segment of the Sunda subduction zone. The range of Sa in Padang is between 0.2 g to 1.1 g for the period below 1 s (Figure 7A). Moreover, the PGA values (Figure 7B) is at the interval of 0.3 g to 0.9 g with the median of about 0.5 g. Using the simulated response spectra from those 100 earthquake scenarios, the TES vulnerability is assessed. Figure 8 presents the three kinds of exceedance probability of damage states; blue dots correspond to extensive damage state, black dots correspond to complete damage state, and red dots represent the sum of these two probabilities. A 50% probability line is drawn to indicate the threshold of safe building that is considered in this study. Figure 8 indicates that the TES may be operational for evacuation because ~95% from the total of 100 earthquake simulations produce less than 50% exceedance probability of the combined extensive-complete damage states. Moreover, most of the cases result in less than

25% probability of exceedance above the extensive damage state. Subsequently, the TES may be considered to be safe for evacuation after the ground shaking and hence, the tsunami vulnerability assessment can be carried out.

Fourth, the tsunami vulnerability assessment is performed. Using the maximum inundation depths at all 23 TES from the 100 earthquake scenarios of the M_w 9.0, the probability of exceeding the severe damage state (DST3) for each TES is calculated. When the chance of severe tsunami damage exceeds 50%, the TES is considered to be not usable as tsunami evaluation building. The probabilities of severe damage for the shelter numbers 16 and 17 are relatively large, i.e. 30% and 36% of the 100 events, and hence, these two shelters may be considered to be unsafe for the evacuation. Moreover, the probabilities of severe damage for the other shelters are relatively small (less than 25%). Therefore, except for the shelter numbers 16 and 17, the rest of the shelters are considered to be operational for evacuation.

Subsequently, the estimation of TES building capacity is evaluated. This may capture another point of view regarding the adequacy of existing TES for evacuation. In terms of capacity, except for shelters numbers 16 and 17, all TES buildings can be used for vertical evacuation during the 10th rank event. However, for the 50th percentile case, the shelter number 1 (sport center of UNP) may not be operational, whilst for the 90th percentile case, shelter numbers 1 and 15 (Elementary school of 24 Padang) are unable to accommodate evacuees since all floors will be inundated. Note that, for the shelter number 1, there is only one floor since most of the building areas are used for the sport arena. In terms of capacity, for the 50th and 90th rank cases, the possible maximum capacity to be accommodated at all TES buildings are only about 64,000 and 41,000 people, respectively. These numbers are insufficient in comparison to the total population in the coastal region of Padang (i.e. ~200,000 people). Therefore, it is highly recommended to increase the number of TES near the coastal areas in Padang. Importantly, the TES assessment results highlight that the stochastic tsunami simulation method is able to capture the uncertainty of the future tsunamigenic impacts and hence, is essential to use this method for developing an effective tsunami mitigation plan.

C2: Explain the choice of the magnitudes (8.5-8.75-9) for the stochastic simulations. Does it mean that for lower values no tsunamis are generated?

Answer:

We used M_w 8.5 as the minimum scenario magnitude in our study because the tsunami hazard produced from the magnitudes less than this level, e.g. M_w 8.25 and M_w 8.0, are considered to be relatively small (below 1 m wave height in the coastal areas; McCloskey et al., 2008; Muhammad et al., 2016). From Figure 1 in this document, we see the relatively minor effects in Padang due to M_w 8.5 tsunami . It shows the tsunami wave heights at three stations, i.e. Tabing, Purus, and Teluk Bayur, at a depth of 5 m. The median wave heights produced from 100 tsunamigenic scenarios are about 1 m which is small and will have minor impact on land (see Muhammad et al., 2016). The impact becomes more insignificant if we consider the M_w 8.25 scenario. Therefore, we choose the M_w 8.5 as the minimum magnitude scenarios.

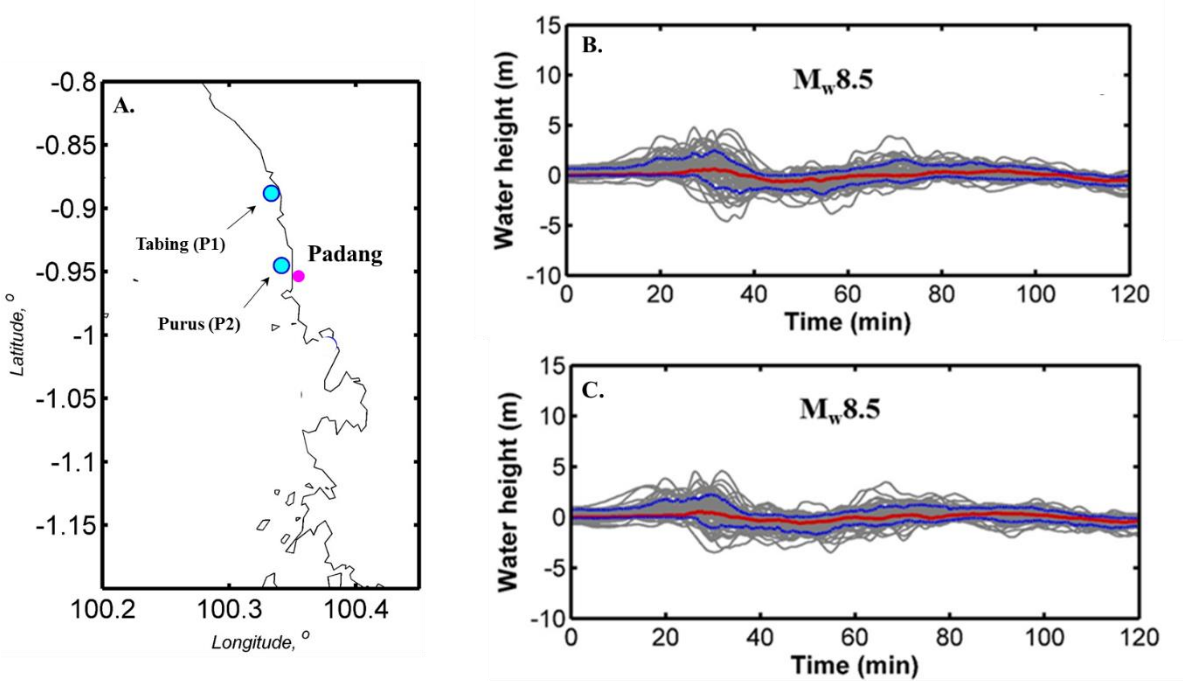

Figure 16. Tsunami wave height profile near coastal line of Padang: (A) site location. (B). Tabing (P1) station). (C). Purus (P2) station.

For the maximum scenarios (i.e. M_w 9.0), it was selected based on the existing research studies from geodetic, paleogeodetic, and paleotsunami investigations. These studies indicated that the accumulated slip in the Mentawai segment of the Sunda subduction zone may generate the tsunamigenic earthquake with the magnitude ranging from M_w 8.8 to M_w 9.0 (Zachariasen et al., 1999; Natawidjaja et al., 2006; Sieh et al., 2008). We did not consider a extreme scenario like the 2004 Indian Ocean tsunami (which is very long) because the tsunami sediment records in North of Sumatra indicated that the recurrence time of destructive tsunamis from the Aceh-Andaman sources is at least 600 years in comparison to ~200 years for the Mentawai segment (Natawidjaja et al., 2006; Monecke et al., 2008) and hence, the M_w 9.0 consider to be more likely than the scenarios such as the 2004 Indian Ocean tsunami. However, such long ruptures are a possibility in the Mentawai segment – we simply did not consider such an assumption.

Based on Reviewer's recommendations, we have added to the methodology section of the revised manuscript the following descriptions regarding the choice of our magnitude scenarios in the revised manucript as follows:

The magnitude M_w 8.5 is used as the minimum scenario because the tsunami hazard produced from the magnitude below this level, e.g. M_w 8.25 and Mw 8.0, is relatively small (less than 1 m wave height in the coastal areas; see Muhammad et al., 2016). The maximum magnitude scenario (M_w 9.0) is selected based on geodetic, paleo-geodetic, and paleo-tsunami studies (Zachariasen et al., 1999; Natawidjaja et al., 2006; Sieh et al., 2008); they indicated that the accumulated slip in the Mentawai segment of the Sunda subduction zone may generate the tsunamigenic earthquake with the magnitude range from M_w 8.8 to M_w 9.0.

C3: Provide some more details on tsunami numerical simulation (finite difference? Inundation with moving boundary?)

Answer:

Agreed. We have added the detail regarding numerical simulation in the revised manuscript which are the following:

A finite-difference method incorporating staggered leap-frog scheme is adopted to solve the governing equations (Goto et al., 1997). In addition, in Goto et al. (1997) code the moving boundary approach developed by Iwasako and Mano (1797) is used for inundation modelling.

C4: The paper refers to the 1797 event when reconstructing the fault geometry: for sure, it is one of the most reasonable mechanism, but it is not the only one and different events with different characteristics can produce different tsunamis.

Answer:

Agreed. The geodetic, paleogeodetic, and paleotsunami studies confirmed that two significant tsunamigenic events occurred in 1797 and 1833 events (Natawidjaja et al., 2006; Sieh et al., 2008; Philibosian et al., 2014) and hence, the scenario may not only follow the 1797 event. We absolutely aware that the possible event from the 1833 source may occur as well. Moreover, a significant tsunamigenic event generated from any point in the Sunda subduction zone is also possible. However, current literature has suggested that the tsunamigenic event from the 1797 scenario may produce the most devastating effects in Padang areas (Borrero et al., 2006;

Natawidjaja et al., 2006; McCloskey et al., 2008; Muhari et al., 2010,2011; Griffin et al., 2016). The historical record regarding the effects of the 1833 and the 1797 events in Padang also confirmed that the 1797 produce more damage than the 1833 event (Natawidjaja et al., 2006). Subsequently, since we consider the worst scenario for the future event, the 1797 event is chosen.

We have a short description regarding the reason of choosing this scenarios in the revised manuscript:

Note that the 1797 event was found to produce more significant tsunami impacts in Padang than the 1833 event (Borrero et al., 2006; Natawidjaja et al., 2006; McCloskey et al., 2008). Consequently, in this study, the 1797 asperity zone is adopted to generate the future stochastic earthquake source models.

C5: The probabilistic approach surely presents some advantages with respect to the deterministic one, taking into consideration also different possible features that the second cannot contemplate, but suffers from some main limitation: first of all, it can be applied only in coastal areas with a detailed knowledge of the seismic structures and a populated seismic and tsunami catalogue. Please mitigate in general the sentences concerning the probabilistic vs deterministic approaches, highlighting also the problems of the first. The text repeatedly reminds that the deterministic approach produces oversimplification, but this is true for over-simplified applications of this methodology, not meaning that the whole procedure is wrong.

Agreed. We have added the following texts to outline this problem:

In the past, two types of earthquake source scenarios have been mainly considered to develop tsunami risk mitigation plans in Padang: deterministic scenarios (Borrero et al., 2006; Schlurmann et al., 2010; Muhari et al., 2010, 2011) and probabilistic scenarios (McCloskey et al., 2008; Griffin et al., 2016). These two methods have both advantages and disadvantages. For instance, the deterministic approach is more communicable to the authorities for developing post-disaster recovery and mitigation plans (McGuire, 2001). However, implementation of deterministic scenarios may oversimplify the tsunami hazards and risks, leading to imprecise mitigation plans (Mueller et al., 2014; Griffin et al., 2015). On the other hand, the probabilistic scenario approach requires the proper consideration of regional earthquake characteristics, including uncertainties in size of the rupture plane and spatial heterogeneity of earthquake slip. Therefore, extensive and detailed data regarding the regional seismological characteristics are essential to develop the probabilistic scenarios. In the previous investigations, those regional earthquake characteristics have not been taken into account properly.

Answer:

C6: How do you expect authorities should use such probabilistic results? Can a decision-makers deal with scientific concepts like probability?

Answer:

The work in this manuscript is a preliminary step to implement into more practical implementation for a disaster risk reduction. The following works that may be carried out in the near future regarding our methodology is Probabilistic Tsunami Hazard Analysis (PTHA) in Padang, Indonesia considering the stochastic tsunami simulation. The PTHA may produce the tsunami hazard maps showing the annual probability of experiencing a tsunami with a specific tsunami intensity hazard, e.g. height, depth and velocity, and may be defined with certain return period. Through this approach, we may effectively use to communicate with the authorities for improving the tsunami mitigation systems in Padang, Indonesia. Moreover, several preliminary works regarding the PTHA using the stochastic tsunami simulation have been successfully implemented in Japan and Mexico (De Risi et al., 2016 and Mori et al., 2017) and hence, it is possible to produce such results.

C7: Figures 9 to 12: what is intended for “inundation height in the coastal line”? Is it the height of the wave on the coast, before land flooding? Or is it the maximum inland elevation reached by the water? In the first case it should be addressed as “maximum wave height on the coast”, in the second it is simply “run-up height”. Please clarify this point.

Answer:

It is the maximum wave height on the coast. We have corrected in the revised manuscript: instead of only the inundation height along the coastal, we have changed to the maximum wave height on the coast.

C8: Line 338: is the Padang population referred to an average value? Does this esteem take into account tourist period, seasonal variation and so on?

Answer:

It is only the average value of Padang population without considering other condition, e.g. tourist period.

Subsequently, we have added these texts into the revised manuscript:

Noted that, the capacity (in persons) of the TES calculated in this study only consider the average population number of Padang excluding other conditions, e.g. tourist period and seasonal variation.

Lines

C9: TECHNICAL CORRECTIONS

(1) Instead of using the word “depth” when referring the water column, use “flow depth”. Agreed. It has been changed accordingly.
(2) Line 43: Mueller et al paper year is 2015, not 2014 (ok in references)
(3) Line 78: “improve” instead of “improving” Line 160: “basing” instead of “based”
(4) 372-3: “. . . to estimate the tsunami hazard level in Padang adopting three magnitude scenarios (Mw 8.5, Mw 8.75, and Mw 9.0)
(5) ” FIGURES 3 to 8: use different palettes for the different figures, addressing different quantities (slip, land elevation, elevation difference, inundation-tsunami depth), it can create confusion.

Answer:

Agreed. The technical corrections have been included in the revised manuscripts.

References

Abrahamson, N., Gregor, N., and Addo, K.: BC hydro ground motion prediction equations for subduction earthquakes. Earthquake Spectra 32, 23–44. doi: 10.1193/051712EQS188MR, 2016.

Ahmad, S., Kyriakides, N., Pilakoutas, K., Neocleous, K., and Zaman, Q. : Seismic fragility assessment of existing sub-standard low strength reinforced concrete structures, Earthq. Eng. Eng. Vib., 14, 439. https://doi.org/10.1007/s11803-015-0035-0, 2015.

Applied Technology Council, : Seismic Evaluation and Retrofit of Concrete Buildings, Report ATC 40, November, 1996.

Aulia, Y. G.: Capacity assessment of tsunami evacuation shelters in Padang city, Thesis, Universitas Andalas, Padang, Indonesia, 2016 (Text in Bahasa).

Bazzurro, P, Cornell, C. A., Menun, C, and Motahari, M.: Advanced seismic assessment guidelines, Pacific Earthquake Engineering Research Centre, Stanford University, 2006.

Briggs, R.W., Sieh, K., Meltzner, A.J., Natawidjaja, D., Galetzka, J., Suwargadi, B., Hsu, Y., Simons, M., Hananto, N., Suprihanto, I., Prayudi, D., Avouac, J.P., Prawirodirdjo, L., and Bock, Y. (2006). Deformation and slip along the Sunda megathrust in the great 2005 Nias-Simeulue earthquake. Science 311, 1897–1901. doi:10.1126/science.1122602.

Borrero, J. C., Sieh, K., Chlieh, M., and Synolakis, C. E.: Tsunami inundation modeling for western Sumatra, Proc. Nat. Acad. Sci. U.S.A., 103, 19673–19677, doi:10.1073/pnas.0604069103, 2006.

De Risi, R. and Goda, K.: Probabilistic Earthquake–Tsunami Multi-Hazard Analysis: Application to the Tohoku Region, Japan. Front. Built Environ., 2, 25, doi: 10.3389/fbuil.2016.00025, 2016.

Douglas, J and Gkimprixis, A.: Using targeted risk in seismic design codes: a summary of the state of the art and outstanding issues, 6th National Conference on Earthquake Engineering and 2nd National Conference on Earthquake Engineering and Seismology, Bucharest, Romania, 14/06/17 - 17/06/17, 3-10, 2017.

FEMA (Federal Emergency Management Agency) 356: Pre-standard and commentary for the seismic rehabilitation of buildings, Federal Emergency Management Agency, Washington, D.C., 2009.

HAZUS. Multi-hazard Loss Estimation Methodology Earthquake Model. Federal Emergency Management Agency, Washington, D.C., 2003.

Iwasaki, T. and Mano, A.: Two-dimensional numerical computation of tsunami run ups in Eulerian description, Proc. Of 26th Conference on Coastal Engineering, Japan, JSCE, 70-74, 1979.

Kurniawan, A. A., Sutikno, S., and Rinaldi: Evaluasi Kapasitas Shelter Evakuasi Untuk Bencana Tsunami Di Kota Padang Berbasis Sistem Imformasi Geografis (SIG), Journal Online Mahasiswa, 1, 1-9, 2014.

Meltzner, A.J., Sieh, K., Abrams, M., Agnew, D. C., Hudnut, K.W., Avouac, J.P., and Natawidjaja, D. H. (2006). Uplift and subsidence associated with the great Aceh-Andaman earthquake of 2004. J. Geophys. Res. 111, B02407, doi:10.1029/2005JB003891.

Monecke, K., Finger, W., Klarer, D., Kongko, W., McAdoo, B. G., Moore, A. L., and Sudrajat, S.U. (2008). A 1,000-year sediment record of tsunami recurrence in northern Sumatra. Nature 455, 1232–1234. doi:10.1038/nature07374.

Mori N, Muhammad A, Goda K, Yasuda T and Ruiz-Angulo A (2017) Probabilistic Tsunami Hazard Analysis of the Pacific Coast of Mexico: Case Study Based on the 1995 Colima Earthquake Tsunami. Front. Built Environ. 3:34. doi: 10.3389/fbuil.2017.00034.

Muhari, A., Imamura, F., Koshimura, S., and Post, J.: Examination of three practical run-up models for assessing tsunami impact on highly populated areas, Nat. Hazards Earth Syst. Sci., 11, 3107-3123, doi:10.5194/nhess-11-3107-2011, 2011.

Muhari, A., Imamura, F., Natawidjaja, D. H., Diposaptono, S., Latief, H., Post, J., and Ismail, F.A.: Tsunami mitigation efforts with pTA in West Sumatra Province, Indonesia. J. Earthq. Tsunami, 4, 341–368, doi:10.1142/S1793431110000790, 2010.

Natawidjaja, D.H., Sieh, K., Chlieh, M., Galetzka, J., Suwargadi, B.W., Cheng, H., Edwards, R.L., Avouac, J.P., and Ward, S.N. (2006). Source parameters of the great Sumatran megathrust earthquakes of 1797 and 1833 inferred from coral microatolls. J. Geophys. Res. 111, B06403, doi:10.1029/2005JB004025.

Rossetto, T. and Elnashai, A.: Derivation of vulnerability functions for European-type RC structures based on observational data, Eng. Str., 25, 1241-1263, 2003.

Sarabandi, P., Pachakis, D., King, S., and Kiremidjian, A.: Empirical fragility functions from recent earthquakes. The 13th world conference in Earthquake Engineering, Vancouver, Canada, August 1-6, 2004.

Sengara, I. W, Sidi, I. D, Mulia, A, Muhammad, A, and Daniel H.: Development of risk coefficient for input to new Indonesian seismic building codes. Journal of Engineering and Technological Sciences, 48, 49–65, 2016.

Sieh, K., Natawidjaja, D.H., Meltzner, A.J., Shen, C.C., Cheng, H., Li, K.S., Suwargadi, B.W., Galetzka, J., Philibosian, B., and Edwards, R.L. (2008). Earthquake super cycles inferred from sea-level changes recorded in the corals of West Sumatra. Science 322, 1674–1678. doi:10.1126/science.1163589.

Wijayanti, E, Kristiawan, S. A, Purwanto, E, and Sangadji, S.: Seismic Vulnerability of Reinforced Concrete Building Based on the Development of Fragility Curve: A Case study, Applied Mechanics and Materials, 845, 252-258, 2015.

Zachariasen, J., Sieh, K., Taylor, F.W., Edwards, R.L., and Hantoro, W.S. (1999). Submergence and uplift associated with the giant 1833 Sumatran subduction earthquake: Evidence from coral microatolls. J. Geophys. Res. 104, 895–919.